Adsorption of CO 2 and Ar on glass surfaces. Computer simulation and experimental study

V. A. Bakaev, W. A. Steele, T. I. Bakaeva, and C. G. Pantano

Citation: The Journal of Chemical Physics **111**, 9813 (1999); doi: 10.1063/1.480329
View online: http://dx.doi.org/10.1063/1.480329
View Table of Contents: http://scitation.aip.org/content/aip/journal/jcp/111/21?ver=pdfcov
Published by the AIP Publishing

Adsorption of CO_2 and Ar on glass surfaces. Computer simulation and experimental study

V. A. Bakaev and W. A. Steele
Department of Chemistry, 152 Davey Laboratory, Pennsylvania State University, University Park, Pennsylvania 16802

T. I. Bakaeva and C. G. Pantano
Department of Materials Science and Engineering, Pennsylvania State University, University Park, Pennsylvania 16802

(Received 20 April 1999; accepted 8 September 1999)

Isotherms of adsorption of CO_2 and Ar are simulated by the grand canonical Monte Carlo on four model surfaces of amorphous silica. The surfaces designated *A* through *D* differ progressively in their degree of annealing, *A* being an unannealed, nonequilibrium surface and *D* being the most extensively annealed. The gas–gas interaction potentials for both gases were taken from the literature and the gas–solid interactions were modeled by applying Lorentz–Berthelot combining rules to the gas–gas potentials plus the TTAM representation of the atom–atom interactions in the solid. The simulated isotherms of Ar on surfaces *A* and *D* are close to each other and to the experimental isotherm for nonporous silica. In contrast, the simulated isotherms and isosteric heats of adsorption of CO_2 on these surfaces differ considerably from each other. This leads to the conclusion that argon adsorption is not sensitive to the changes in surface structure that occur during annealing, but CO_2 is. Since these gases differ considerably in their polarity, these results indicate that the observed differences in adsorption behavior are due in large part to the annealing-induced changes in the electrostatic part of the CO_2–SiO_2 interaction. The isotherm of CO_2 on *D* was made to be very close to an experimental isotherm on dehydroxylated nonporous silica by diminishing the electrostatic part of the CO_2–SiO_2 interaction by 30% from that in the original model of the potential. Isotherms of adsorption of CO_2 on multicomponent glass fibers measured at 194.5 K are reported here. The sub-monolayer experimental isotherms on glass lie higher than an isotherm on hydroxylated silica which in turn lies higher than that for dehydroxylated silica. The sensitivity of the physical adsorption of CO_2 to the chemical nature and the structure of the SiO_2 surface indicates that comparisons of experiment with simulations of the isotherms of polar or quadrupolar molecules like CO_2 on such model surfaces can be a useful probe of surface structure of silica and silicate glasses. © *1999 American Institute of Physics.* [S0021-9606(99)70445-9]

I. INTRODUCTION

A knowledge of the atomic structure of silicate glasses is basic for understanding their properties on an atomic level. Thus, the structure has been studied for more than 60 years, primarily by x-ray and neutron diffraction.[1] Those studies provide a solid foundation for extensive computer simulations of silicate melts and glasses.[2] These x-ray and neutron elastic scattering experiments give the radial distribution functions (RDFs) which can be compared with RDFs obtained from computer simulations. However, there appears to be no direct experimental information on RDFs at the surface of amorphous silica or silicate glasses. Thus the experimental data that validate bulk silica simulations do not exist for amorphous silica surfaces and one has to use more circumstantial evidence. For example, quantitative simulation results for the amorphous silica surface[3] can be compared with experimental data for the concentration of surface silanol groups (Si–OH) which has been measured for many silicas by FTIR.[4] Because the simulated surface did not contain OH-groups, it was assumed that silanols would exist at dangling bonds or strained siloxane sites.[3] Of course, the number of these sites on the simulated surface depends significantly upon the annealing process used in the simulation which takes the system from the fractured surface often used as a starting point to the hydrophobic surface obtained in the limit of the fully annealed, room temperature system. The example illustrates the typical situation in the computer simulation of silicate glass surfaces: experimental data that can be used to validate the simulations are scarce and it is likely that in all cases, both the experimental and the simulation data will be significantly dependent on the annealing of the surface.

We have proposed[5] to use computer simulation of physical adsorption as a method to check the validity of simulated silica surface atomic structures. Specifically, one would (i) simulate the surface atomic structure, (ii) simulate the isotherm of physical adsorption on a surface with that structure, (iii) compare the simulated isotherm with experimental data to test the validity of the simulated structure that produced the isotherm. Due to the nonequilibrium nature of the annealing process, comparisons should be made as a function of the surface relaxation processes that occur during the experimen-

tal and simulational annealing that bring the system from the limiting condition of an initial planar surface to the fully annealed system. In Ref. 5, we calculated the binding energy of a water molecules at various points over amorphous dehydroxylated silica surfaces. In this way, it was shown that simulated surfaces with significant concentrations of coordination defects (single- and triple-coordinated oxygen atoms) will interact sufficiently strongly with water molecules to create hydrophilic adsorption sites. On the other hand, it was shown that a surface simulated by a method that converts all the surface oxygen atoms into bridging oxygens can be hydrophobic, in agreement with experiment.

In this paper, we are concerned with simulations of submonolayer physical adsorption on silica surfaces simulated previously. The results of the simulations will be compared with each other and with real experimental data in an attempt to demonstrate that useful information about the surfaces of silica can be extracted from such comparisons. Of course, interaction potentials must be modeled realistically for such a procedure to be successful. To this end, atom–atom (or site–site) models were employed in which the total gas–solid interaction was taken to be a pairwise sum over the atoms in the solid and in the gas molecule. Of course, this requires that one know (or guess) the well-depth and size parameters of the site–site interaction functions as well as the locations of the sites. The coordinates of Si and O atoms necessary for an adsorption simulation on several silica surfaces were determined mainly in the previous simulation studies.[5,6] (Those surfaces are briefly described here in Sec. II B.)

As probe molecules we have chosen Ar and CO_2. It will be shown that the simulated adsorption isotherms of Ar do not depend on the detailed atomic structures of the surfaces used here. (cf. Fig. 3). In contrast, the adsorption of CO_2 depends dramatically on the structures of the simulated silica surfaces (cf. Fig. 4) because the model interaction potential of CO_2 includes terms for the interaction of its quadrupolar (and higher) molecular moment with the structure-dependent electrostatic field at the silica surface. It will be argued that comparison of these simulated isotherms with each other and with experiment can be used to validate the atomic structure of the simulated silica surfaces.

Details of the model interaction potentials for molecules adsorbed on silica are described in Secs. II A and II D. The potentials consist of a van der Waals part made up of Lennard-Jones (LJ) functions and an electrostatic part (the latter only for CO_2). The LJ-component is empirical but we take its parameters from independent computer simulations of rare gases adsorbed on silicalite. The electrostatic component depends on charges ascribed to C and O atoms in a CO_2 molecule as well as effective charges ascribed to the Si and O atoms in silica. We took charges on the atoms of a CO_2 molecule that reproduce the experimental quadrupole moment (see Sec. II D). As to the effective charges on the atoms of silica, they were initially taken to be those of the TTAM model for the atomic interactions in the bulk.[7] Since this produced simulated adsorption somewhat in excess of the the experimental values, the electrostatic part of the interaction was diminished by 30% (see Sec. II D) to give simulated adsorption that does match experiment. The adjusted effective charges were then used to simulate isotherms of CO_2 on different simulated surfaces. The experimental data that we compare with our simulations were taken from the literature. These are isotherms of adsorption of Ar and CO_2 on nonporous high surface area silica.[8,9] We were also able to obtain differential heats of adsorption for these systems from the simulations. In one case, these could be compared with experimental results.

The isotherms of CO_2 on pure dehydroxylated silica have also been compared with those on the surfaces of glass fibers of complex composition that were measured in this work. This comparison shows that one can use simulated isotherms of CO_2 to probe the structure of simulated silica surfaces and, by comparison with real isotherms, to probe the structure of real silicate glass surfaces.

II. MODELS AND METHODS

A. General

Adsorption was simulated in this paper by the grand canonical Monte Carlo algorithm as described in Refs. 10 and 11. This method takes activities of the gas in equilibrium with the molecules adsorbed on the surface of interest at a specified temperature as input data. The gas phase activity z was calculated from a three-term virial expansion:[12]

$$z = \frac{P}{kT} + B\left(\frac{P}{kT}\right)^2 + \frac{1}{2}C\left(\frac{P}{kT}\right)^3. \tag{1}$$

Here P is the pressure of a gas in equilibrium with adsorbed molecules; and B and C are its second and third virial coefficients. The input data in these simulations were not pressures but relative pressures P/P_0. The reason is that the molecules adsorbed on model silica surfaces in the simulations are not real but models determined by their interaction potentials. Their thermodynamic properties—including the dependence of saturation vapor pressure P_0 and virial coefficients in Eq. (1) on temperature—are known from computer simulations (see Secs. II C and II D) and are substituted for the properties of real molecules. In this situation, adsorption vs relative pressure is more appropriate than adsorption vs pressure since the former takes account of the difference in the values of P_0 for the real and model molecules. The same is true for the virial coefficients in Eq. (1) but for the pressures used in these simulations they give only very small corrections to the first (ideal gas) term.

A peculiarity of this simulation is that the simulation box was not of cubic or rectangular shape as usual but possessed a wavy bottom that is almost coincident with the shape of the adsorbing surface. This is because that surface deviates considerably from a plane. This was shown by constructing a projection of the surface onto an XY plane divided into 40×40 square elements. In the center of each element, the position $Z_{\min}$ of an Ar atom that has the minimum energy of interaction with the substrate was determined. The surface $Z_{\min}(X,Y)$ that results has the profile shown in Fig. 1.

One of the moves in the grand canonical ensemble Monte Carlo is insertion of a particle in a random position in the simulation box. To perform such a move we choose X

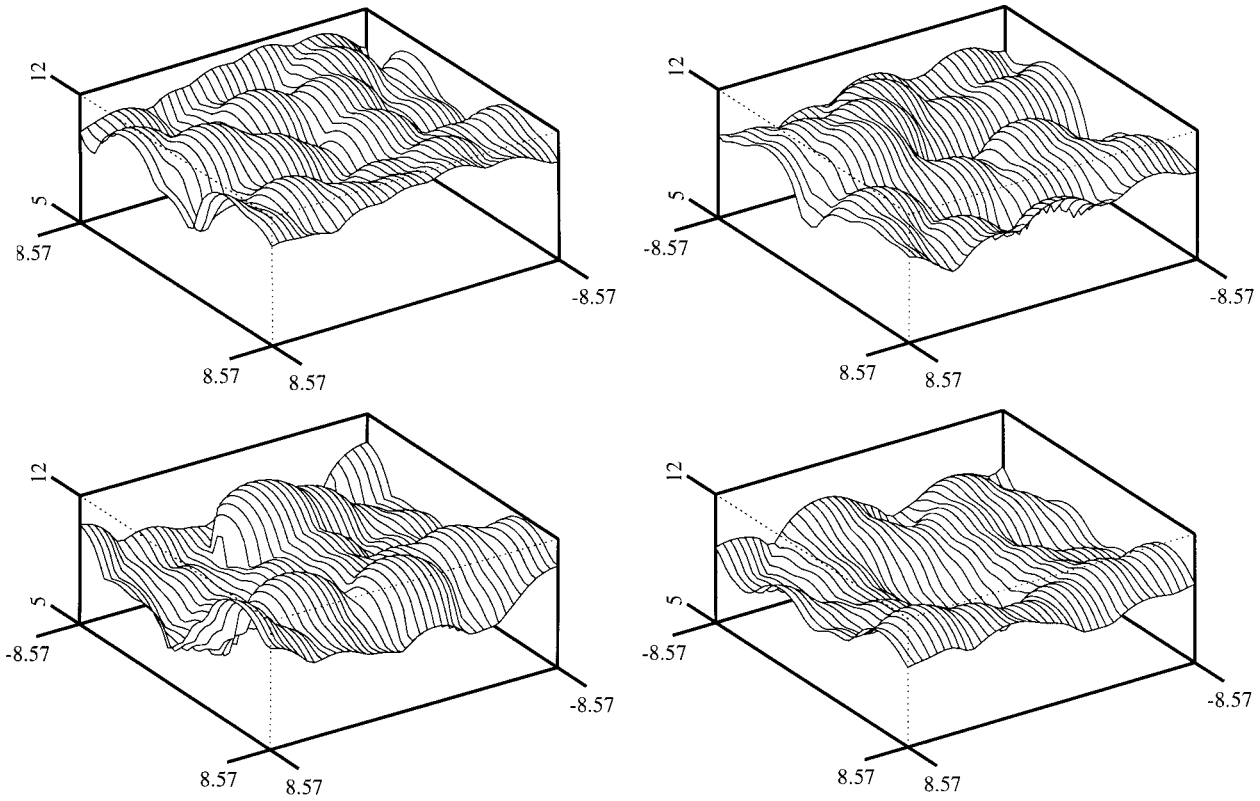

FIG. 1. Profiles of simulated surfaces: top left: Surface *A*; bottom left: Surface *B*; top right: Surface *C*; bottom right: Surface *D*. All distances are in Å.

and Y at random, as usual, then determine into which element the point (X,Y) falls. The insertion move is generated by choosing Z at random from a uniform distribution between $Z_{\min}(X,Y)-\Delta Z$ and $Z_{\min}(X,Y)-\Delta Z+H$ where ΔZ and H are constants. Thus the simulation box consisted of 40×40 square prisms of the same height H. In this way, the top of the box was a wavy surface that was parallel to the bottom. The values of ΔZ and H were chosen to be such that the density of adsorbate at the bottom and the top of simulation box be negligibly small.

Examples of the density profiles for three sub-monolayer coverages of CO_2 is shown in Fig. 2. These were obtained with $\Delta Z=2$ Å and $H=12$ Å. This picture was obtained by evaluating the X and Y coordinates of the C-atom in each adsorbed CO_2 molecule. The profiles also determine $Z_{\min}(X,Y)-\Delta Z$—the bottom of the corresponding prism. (The heights of all the prisms H were divided into 40 parts which determine 40 bins of a histogram.) The molecule was assigned to the bin corresponding to the distance of the C-atom Z-coordinate from the bottom of the prism. Thus the ordinate of Fig. 2 is the average density in a thin wavy layer that is the sub-monolayer film and thus has the same shape as the adsorbing surface as presented in Fig. 1.

Another peculiarity of this simulation is that the area of adsorbing surface obtained from the simulations of the solid was rather small to give useful adsorbed phase properties. The edge length of the initial (bulk) simulation box in the X and Y directions was only 17.6 Å (in Fig. 1 it is smaller by the edge of the 40×40 mesh element) so that the projection of the surface on the XY-plane has an area of 309.8 $Å^2$. Since the molecular area of CO_2 is about 20 $Å^2$,[9] the monolayer capacity of this surface is only 15.5 molecules. Since this might be too small for reliable simulations of the adsorption isotherm, we increased the area of the adsorption simulation box by 9 times by extending the periodic boundary conditions. Thus, the surface was enlarged by creating a 3×3 larger area made up of the original element plus one neighboring image in each of the plus and minus X and Y directions so that the potential surface repeats itself 9 times inside the augmented simulation box. Even though the simulated

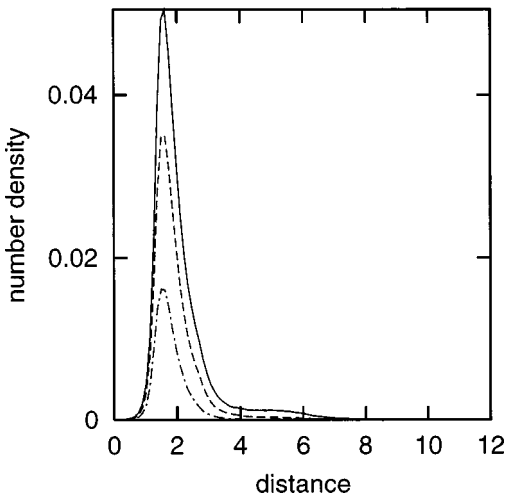

FIG. 2. Density profiles of adsorbed carbon dioxide for the isotherm designated by error bars in Fig. 4. Solid line: $P/P_0=0.5$; dashed line: $P/P_0=0.3$; dotted–dashed line: $P/P_0=0.1$. Distance is in Å, number density is in $Å^{-3}$.

solid is repeated inside this box, the adsorbed molecule images are located only outside of it.

The energy of interaction of an adsorbed molecule with the substrate includes the van der Waals component which is assumed to be the sum of pairwise interactions with the substrate atoms. To calculate this energy for a molecule located at any point we describe a sphere of radius R around this point. The interaction of a molecule with all the atoms of adsorbent inside this sphere are calculated by the summation of Lennard-Jones (LJ) energies from separate atoms of a molecule (if a molecule is composed of more than one atom):

$$U=4\sum_{\alpha,\beta}\epsilon_{\alpha\beta}\left[\left(\frac{\sigma_{\alpha\beta}}{r_{\alpha\beta}}\right)^{12}-\left(\frac{\sigma_{\alpha\beta}}{r_{\alpha\beta}}\right)^{6}\right], \tag{2}$$

where $r_{\alpha\beta}$ is the distance between the atom α in a molecule and an atom β of adsorbent and $\epsilon_{\alpha\beta}$ and $\sigma_{\alpha\beta}$ are LJ parameters which depend on the types of interacting atoms. Interactions with substrate atoms outside the sphere are calculated in the assumption that a continuous medium of number density n_β fills the half-space below the plane $z=\langle z\rangle$ so that the long-range part of the energy is given by

$$\Delta U=\sum_{\alpha,\beta}\Delta U_\beta(z_\alpha),$$

$$\Delta U_\beta(z_\alpha)=-4\epsilon_{\alpha\beta}\sigma_{\alpha\beta}^6 n_\beta\pi\left(\frac{1}{6R^3}+\frac{\langle z\rangle-z_\alpha+R}{2R^4}\right)$$

if $\langle z\rangle-z_\alpha+R>0$, otherwise

$$\Delta U_\beta(z_\alpha)=-4\epsilon_{\alpha\beta}\sigma_{\alpha\beta}^6 n_\beta\pi\frac{1}{6(z_\alpha-\langle z\rangle)^3}. \tag{3}$$

Here $\langle z\rangle$ is the arithmetic mean of the 1600 values of $Z_{\min}$ mentioned above minus the LJ-parameter σ for Ar (see Sec. II C); R is 8.8 Å—half of the edge of the bulk (surface) silica simulation box, and n_β is the number density of Si or O in the bulk. It has been checked that direct application of Eq. (2) to all the atoms of the surface layer gives practically the same isotherms as those using this calculation.

Values of the parameters $\epsilon_{\alpha\beta}$ and $\sigma_{\alpha\beta}$ were evaluated by the Lorentz–Berthelot rule

$$\epsilon_{\alpha\beta}=\sqrt{\epsilon_{\alpha\alpha}\epsilon_{\beta\beta}};\ \sigma_{\alpha\beta}=(\sigma_{\alpha\alpha}+\sigma_{\beta\beta})/2. \tag{4}$$

Thus, ϵ for the interaction of an O-atom in a CO_2 molecule and an O-atom in silica requires that one know the values of ϵ for the O–O interaction between O-atoms in CO_2 molecules and between O-atoms in silica. The former is taken from the previous simulations of bulk CO_2 (see Sec. II D). The latter comes from potentials used in adsorption simulations of simple gases in zeolites *A*, *X*, *Y*, and silicalite.[13] The LJ-parameters for the site–site interactions in silicalite were taken from Table II of Ref. 13: $\epsilon_{11}/k=101.6$ K, $\sigma_{11}=2.708$ Å and $\epsilon_{22}/k=18.6$ K, $\sigma_{22}=0.677$ (1 stands for O, 2 stands for Si). These parameters produced reasonable agreement between simulated and experimental isotherms of adsorption of Ar, O_2, and N_2 in silicalite (cf. Figs. 1–3 of Ref. 13).

The grand canonical ensemble Monte Carlo simulation gives not only the average number of particles in the simulation box $\langle N\rangle$ but their average potential energy $\langle E\rangle$ as well. After correcting for the number of unadsorbed molecules in the box, these data can be employed to determine the isosteric heat of adsorption:[14]

$$q^{st}=\partial\langle E\rangle/\partial\langle N\rangle+RT. \tag{5}$$

The numerical differentiation was performed with the help of a cubic spline interpolation.[15] The standard deviations as depicted in Fig. 5 were determined by the method of Monte Carlo simulations of synthetic data sets.[15] For each value of $\langle N\rangle$ and $\langle E\rangle$ their standard deviations $\delta\langle N\rangle$ (shown for one curve in Fig. 4) and $\delta\langle E\rangle$ were determined by the Flyvbjerg and Petersen block average method.[11] Then synthetic data sets were simulated by sampling N and E from independent gaussian distributions with the above mentioned averages and standard deviations. Each of these data sets gives an independent plot of q^{st} vs N. (These plots allow one to determine averages and their confidence limits as shown in Fig. 5.)

B. Model surfaces

This paper is devoted to simulations and measurements of the physical adsorption of Ar and CO_2 on silica and silicate glass samples. Tables of coordinates of the atoms in the simulated solids were mainly obtained from simulations of the solid surfaces published elsewhere.[5,6] Surfaces *A* and *B* were generated in this work as in these previous studies. Here, we describe briefly how these model surfaces were obtained to clarify the main differences between them.

The simulations of these solid surfaces started from a conventional molecular dynamics (MD) simulation of the bulk in a cubic box containing 120 Si and 240 O atoms at a density of 2.2 g/cc using periodic boundary conditions (PBC) in the *X*-, *Y*-, and *Z*-directions. The same *ab initio* potential model (TTAM) and Ewald summations of electrostatic potentials were used as in Ref. 16. The system was annealed to a final configuration of a continuous random net of fairly regular SiO_4 corner-sharing tetrahedra. (Details of the annealing process are given in Ref. 5). The periodic boundary condition in the *Z*-direction was then removed. This created the totally unannealed surface A used here. The surface layer consisted of a periodic array of the simulation boxes in the *X* and *Y* directions plus image arrays shifted down in the *Z* direction. This virgin surface contains a large concentration of coordination defects such as single and triple coordinated oxygen atoms.

Surface B was obtained from *A* by an annealing process similar to that used in Ref. 3: The temperature of the surface layer was raised to 1000 K and a conventional MD simulation was carried out for 20 ps to produce annealing. Then the temperature was linearly decreased from 1000 K to 300 K over a time of 20 ps to produce *B*. The concentration of single and triple coordinated oxygen atoms did not change after this annealing.

The surface *C* was the hydrophobic surface modeled in Ref. 5. It was obtained from surface *A* by high temperature annealing starting from 8000 K. The simulation was a com-

bination of MD and Monte Carlo algorithms that did not allow the concentration of the oxygen atoms with coordination other than that of a bridging oxygen to increase. As a result, the surface layer of *C* contains no coordination defects, i.e., it consists of only bridging oxygen atoms and four-coordinated silicon atoms. However, it contains a large concentration of two-membered oxygen rings (edge-sharing tetrahedra). Those edge-sharing tetrahedra are produced when one single coordinated oxygen (≡Si–O) combines its dangling bond with that of a triple coordinated silicon (≡Si·) to form a strained siloxane bridge (≡Si–O–Si≡).

Finally, surface *D* contains neither coordination defects nor edge-sharing tetrahedra and was obtained from surface *A* by very slow annealing with a nonlinear temperature profile that is discussed in detail elsewhere.[6]

C. Argon

In computer simulations of bulk Ar, the Ar–Ar interatomic interactions are usually modeled by Eq. (2) with parameters[17] $\epsilon = 120$ K and $\sigma = 3.40$ Å. The saturated vapor pressure P_0 of this model molecule was obtained in extensive computer simulations of LJ fluids:[18]

$$\ln P^* = 3.0634 - 6.7557/T^*, \tag{6}$$

where $T^* = kT/\epsilon$ and $P^* = P\sigma^3/\epsilon$. At the boiling point of real Ar (87.29 K), this equation gives $P_0 = 632.5$ mmHg while at 89.06 K it gives 760.4 mmHg. Thus the boiling point of our model Ar is 1.8 K higher than that of real Ar.

The second and third virial coefficients in Eq. (1) for our model Ar were not taken from experimental data but evaluated from Tables I-A,E of Ref. 17 for a LJ gas. For the values of *P* and *T* used in this work, corrections to the first (ideal gas) term in Eq. (1) are very small: 0.8% for the second and 0.001% for the third term at the highest *P* in Fig. 3.

D. Carbon dioxide

The EPM model of a CO_2 molecule was used in this work because this model has been previously employed in computer simulations of the liquid–vapor coexistence curve.[19] The model places 0.6645 of an electron charge on the C-atom and two negative charges with half that value on the O-atoms (the C–O bond length is 1.161 Å). It also places the LJ force sites on C- and O-atoms using parameters of Eq. (2) equal to: $\epsilon_{11} = 82.00$ K, $\sigma_{11} = 3.06$ Å; $\epsilon_{12} = 49.06$ K, $\sigma_{12} = 2.92$ Å; $\epsilon_{22} = 29.00$ K, $\sigma_{22} = 2.79$ Å. Here 1 stands for O and 2 stands for C and the mixed parameters ϵ_{12} and σ_{12} were obtained from the combination rule of Eq. (4).

Unfortunately Ref. 19 does not provide reliable $P_0(T)$ data at 194.5 K where our simulations were carried out. However they determined the critical parameters of EPM model CO_2: $T_c = 313.4 \pm 0.7$ K, $P_c = 76.5 \pm 4.5$ bar.[19] To use these data we employed the experimental equation $P_0(T)$ for liquid CO_2:[20]

$$\ln\left(\frac{P_0}{P_c}\right) = a_0\left(1 - \frac{T}{T_c}\right)^{1.935} + \sum_{i=1}^{4} a_i\left(\frac{T_c}{T} - 1\right)^i, \tag{7}$$

where $T_c = 304.21$ K, $P_c = 73.825$ bar and

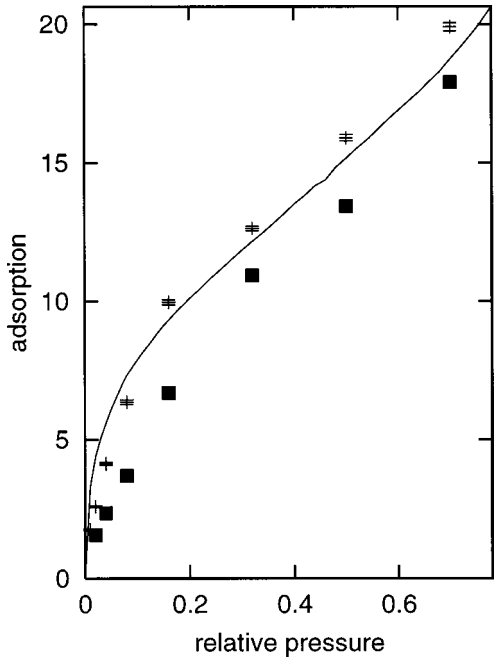

FIG. 3. Simulated and experimental isotherm of adsorption of Ar on vitreous silica at 77 K. Line: Standard isotherm of Ar on nonporous silica (experimental data); filled squares: Simulated isotherm on surface *A*; error bars: Simulated isotherm on surface *D* (the simulation errors are about the same for *A* and *D*). Adsorption is in μmol/m^2.

$$a_0 = 11.377\,371;\ a_1 = -6.884\,9249;\ a_2 = -9.592\,4263;$$

$$a_3 = 13.679\,755;\ a_4 = -8.605\,6439.$$

Here T_c and P_c are the experimental critical temperature and pressure which are somewhat smaller than those given above for the EPM model. To obtain $P_0(T)$ for the EPM model of CO_2 we used Eq. (7) with the experimental values of T_c and P_c replaced by the EPM values given above.

Another problem with Eq. (7) is that the end of its range is the triple point of CO_2: $T = 216.58$ K but the experimental isotherm of CO_2 on dehydroxylated nonporous silica with which our simulated isotherms were compared was measured at 194.7 K.[9] Their results are presented as adsorption vs relative pressure (P/P_0) using not the saturated vapor pressure of solid CO_2 but the extrapolated vapor pressure of supercooled liquid (1.82 atm). If one calculates P_0 at 216.58 K and 280 K by Eq. (7) with experimental values of T_c and P_c and makes a linear extrapolation of $\ln(P_0)$ vs $1/T$, one will obtain $P_0 = 1.818$ atm at 194.7 K which is close to the accepted value in Ref. 9. Direct substitution of $T = 194.7$ into Eq. (7) gives $P_0 = 1.70$ atm. Thus we recalculated the experimental data of Ref. 9 using this value of P_0. This is necessary in these simulations because we have obtained the EPM value P_0 by direct substitution of temperature in Eq. (7).

Experimental values of the second virial coefficient for CO_2 vs *T* are given in Table VI of Ref. 20. The minimum temperature there is 220 K so an extrapolation was made in coordinates $\ln(-B)$ vs $1/T$. Extrapolation to 194.7 K gives $B = -337 \pm 3$ cc/mol. This value was substituted in Eq. (1) but the ratio of absolute value of the second term in Eq. (1) to the first one is only about 1% at the highest pressures used

in the simulations. The third term of Eq. (1) was neglected because it was believed to be very small at the pressures used (cf. Sec. II C).

The simulation technique for CO_2 differs from that of a monatomic molecule in that one has not only to change the position of the center of a molecule in the simulation box but also to change its orientation. The change of the orientation of a molecule was performed here by rotating it by a constant angle around a random axis going through the center of C-atom. The angle was such that the maximum displacements of O-atoms were the same for rotation and shift of the center of a molecule.

Another peculiarity of the CO_2 simulation relative to that of Ar was that one has to calculate not only the short range van der Waals component of the interatomic interaction but also the long range electrostatic component. The electrostatic energies at the C- and O-atoms of a CO_2 molecule were calculated by summing the electrostatic interactions of their charges with the charges of the model O- and Si-atoms contained in the primary simulation box. As usual, the minimum image convention[11] was adopted. The contributions to the electrostatic potential from the periodic images of the surface simulation box were evaluated by the multipole expansion method. It has been checked that their influence on the adsorption isotherm is below the level of statistical errors. The effective charges on the model O- and Si-atoms of silica were -0.8 and 1.6 electron, respectively, which were slightly smaller than those of -1.2 and 2.4 used in the potential model employed in the simulations of the silica atomic structures (bulk and surface). The rationale for this change is explained in Sec. III.

E. Experiment

The experimental results used in this paper consisted of both literature data and those measured in this work. The literature data include an isotherm of adsorption of Ar which was fitted to the equation [Eq. (2) of Ref. 8]:

$$V/S_s^{\mathrm{Ar}} = \alpha_s/3.30 \tag{8}$$

where V is the amount of Ar adsorbed on nonporous silica at 77.2 K expressed in cubic centimeters at S.T.P./gram, S_s^{Ar} is the specific surface of the sample, and α_s is a standard α-curve.[8,14] It has been shown that despite the fact that experimental isotherms $V=V(P/P_0)$ vary from one sample of silica to another, their standard α-curves as well as isotherms expressed per unit area of the sample surface are the same for all nonporous samples and even for mesoporous samples at small coverages.[8,14]

Other experimental isotherms taken from the literature were those of CO_2 on hydroxylated and dehydroxylated nonporous silica at 194.7 K.[9] In addition, some isotherms of CO_2 on glass fibers have been measured experimentally in this work. They were measured volumetrically on a fully automated installation ASAP 2000 (Micromeritics). A liquid thermostat bath was employed to maintain the sample temperature. The mixture of solid CO_2, chloroform, and carbon tetrachloride used in the bath has been reported to maintain temperature at 194.7 ± 0.1 K.[9] The ASAP 2000 is equipped with a gas thermometer that automatically measures P_0 of CO_2. However, this thermometer did not work at the experimental temperature because P_0 was close to the upper limit of the apparatus pressure and the gas did not always condense at the available values. In this case we checked the stability of temperature independently by condensing CO_2 in the empty sample bulb. It was found that this bath maintains temperature at the level 194.5 ± 0.2 K. We used *E*-glass fiber with specific surface 2.5 m^2/g as determined by Kr on ASAP 2000.

III. RESULTS AND DISCUSSION

In this paper, simulations of the adsorption of non-polar argon and quadrupolar CO_2 on four simulated dehydroxylated amorphous silica surfaces are used as probes of surface structure. It has been demonstrated previously that these surfaces differ primarily in the number and nature of the defects associated with nonbridging oxygen surface atoms that give rise to large local electrostatic fields.[5] It was also shown that the density of these defects decreases as the highly defective virgin surface (*A*) is annealed.[6]

For moderate submonolayer coverages, the amount of argon adsorption at a given pressure is insensitive to the density of surface defects (see Fig. 3). Figure 3 shows isotherms for a totally unannealed (virgin) surface *A* that contains 11 singly coordinated oxygens in a simulation box with area $=310$ Å^2 and for the most thoroughly annealed surface *D* for which all surface oxygens are bridging. These two isotherms are close to each other and to the experimental isotherm of Ar on nonporous silica (see Sec. II E). This means that our simulation reproduces the adsorption of argon on the nonporous dehydroxylated silica surface. The simulation is based on empirical LJ interatomic potentials described in Sec. II A. However, the parameters of those potentials were taken from independent sources and were not adjusted in the present simulations. The atomic structure and profiles (cf. Fig. 1) of the surfaces *A* and *D* are different but adsorption of argon is not very sensitive to these differences.

This is clearly not the case for adsorption of CO_2 as shown by Fig. 4. In contrast to the Ar isotherms, the amount of adsorption per unit area at fixed pressure for CO_2 on surface *A* in Fig. 4 is large compared to that on surface *D*. The difference between the behavior of CO_2 and Ar can be traced to the differences in gas/solid interatomic potentials. The potential for a CO_2 molecule on silica includes a pairwise summable LJ part plus an electrostatic part (see Sec. II D) which is of course absent from the argon interaction. Thus, the isotherms of argon and CO_2 on the same silica surfaces in Figs. 3 and 4 differ primarily because of the electrostatic energy of the CO_2 molecules interacting with the electrostatic field at the SiO_2 surface. In previous work, it has been shown that the water-silica interaction is considerably larger on the weakly annealed surfaces *A* and *B* than on the thoroughly annealed surfaces *C* and *D* due to the presence of a large (and irregularly varying) electrostatic field on *A* and *B* (see Sec. II D) that enhances both the CO_2 adsorption and the isosteric heats of adsorption for these systems. The steep drop in the heats with increasing coverage shown in Fig. 5 for surfaces *A* and *B* is characteristic of a highly heteroge-

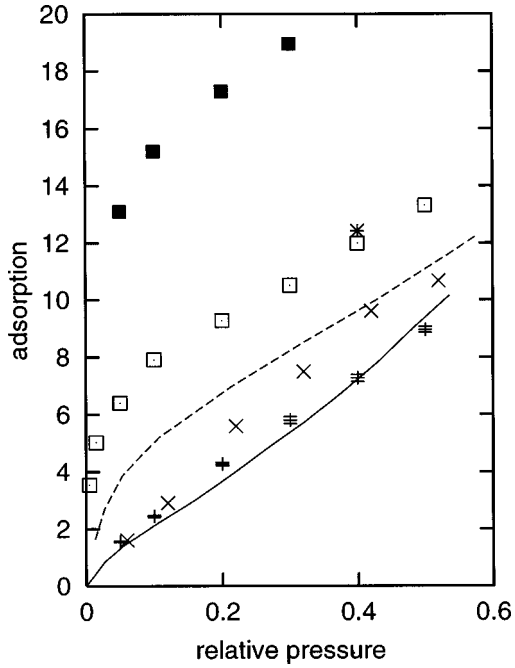

FIG. 4. Simulated and experimental isotherms of adsorption of CO_2 at 194.5 K. Solid line: Experimental isotherm on dehydroxylated nonporous silica; dashed line: Experimental isotherm on hydroxylated nonporous silica; symbols are for simulated isotherms: Filled squares: On surface *A*; open squares: On surface *B*; crosses: On surface *C*; error bars: on surface *D*. *A* point at relative pressure 0.4 designated by the star corresponds to adsorption on the *D* surface with increased effective charges on O- and Si-atoms (see text). Adsorption is in μmol/m^2.

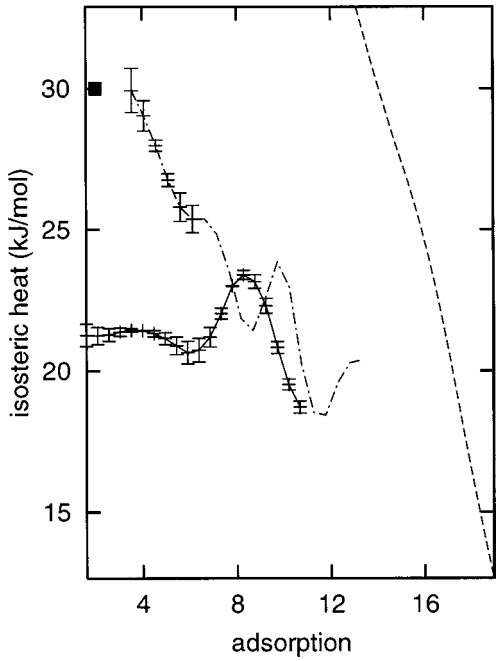

FIG. 5. Isosteric heats of adsorption for CO_2: Solid line with error bars: On surface *C*; dotted–dashed line with error bars: On surface *B*; dashed line: On surface *A*; symbol: experiment on hydroxylated silica gel. Adsorption is in μmol/m^2. Based upon a CO_2 area of 22 Å^2/molecule, the monolayer of CO_2 corresponds to 8 μmol/m^2.

neous surface composed of adsorption sites of different strengths. Based on the water/silica calculations, it is likely that this heterogeneity is due to locally strong CO_2-silica electrostatic interactions. The small and relatively constant isosteric heats for *C* in Fig. 5 indicate that this surface is much more homogeneous than *A*, which is consistent with a relative absence of electrostatic field at the nearly defect-free surface *C*. It is also consistent with our previous finding that the binding energy of a water molecule on the strongest adsorption site of the surface *C* is 4 times smaller than on the strongest adsorption site of a weakly annealed surface similar to *A* or *B* (cf. lines 1 and 6 in Table 1 in Ref. 5). These strong sites are primarily due to the singly and triply coordinated oxygen atoms present at the surface in considerable (and equal) concentrations at *A* and *B*. The defect oxygen atoms generate charged tetrahedra (tetrahedra consisting of bridging oxygen atoms are electroneutral) which are usually strongly distorted.[5] In general, distorted SiO_4 tetrahedra generate strong electrostatic fields that enhance the adsorption energies of dipolar molecules in their vicinities. This must also be true for a quadrupolar CO_2 molecule and this is the reason why the broken curve in Fig. 5 lies so high. It is notable that the heats remain large at coverages up to at least 2 monolayers, probably due to the long-range character of the electrostatic terms.

The simulations for surface *A* lie much higher than the only experimental point in Fig. 5. That point was obtained long ago for a silica gel[21] at a time when the methods of adsorbent characterization were not well developed. The result is referred to in a later paper concerned with the heats of adsorption of CO_2 on various adsorbents other than silica[22] where it is argued that the experimental point in Fig. 5 refers to a sample of a porous hydroxylated silica surface. It is reasonable that this heat is higher than on the nonporous dehydroxylated surface since both porosity and hydroxylation increase the heat of adsorption. The latter can be seen from the comparison of experimental isotherms for hydroxylated and dehydroxylated surfaces in Fig. 4. [A higher isotherm should correspond to higher heats of adsorption (cf. Figs. 4 and 5).]

The fact that the heats of adsorption of CO_2 on the model unannealed surface *A* are much larger than experiment suggests that there are some important differences between the atomic structure of that surface and real silica surfaces. A comparison of the adsorption of CO_2 on surfaces *A* and *B* shown in Figs. 4 and 5 indicates that the adsorption characteristics of these two surfaces are very different, those for the surface *B* being much closer to real silica surfaces than *A*. The latter was annealed at 1000 K which is lower than the glass transition temperature of liquid silica [ca. 1500 K Ref. 16)]. Below the glass transition temperature the structure of glass in the bulk is frozen so that one would not expect large structure changes to take place in the simulated annealing that converts the model surface *A* into *B*. Indeed, the concentration of singly and triply coordinated oxygen atoms (topological structure) of both surfaces is the same but the distortions of the surface tetrahedra (as measured by their dipole and quadrupole moments[5]) will be reduced in the annealing. If so, the electrostatic field at surface *B* will be reduced relative to that for *A*, thus giving a plausible explanation for the

differences in adsorption and heats shown in Figs. 4 and 5 for these two surfaces.

The agreement between the simulated isotherm of CO_2 on the most thoroughly annealed surfaces *C* and *D* and experimental isotherm was achieved by slightly adjusting the model of the CO_2/SiO_2 potential (see Sec. II D). Use of the initial values of -1.2 and 2.4 electron for the charges on O- and Si-atoms in this interaction in the simulation of CO_2 adsorbed on surface *D* gave a point (the star at $P/P_0 \approx 0.4$ in Fig. 4) that is not only considerably higher than the experimental coverage on the dehydroxylated silica surface at the same value of P/P_0 but is even higher than the coverage at this relative pressure on a hydroxylated silica surface. The figures show that considerably better agreement was obtained if these charges were arbitrarily decreased to -0.8 and 1.6 for the O- and Si-atoms for this and the other simulated CO_2 isotherms. A similar adjustment of charges was made in the computer simulation of the isotherms of CO_2 on silicalite NaZSM-5 zeolite[23] where the O- and Si-atoms of silicalite were assigned charges of -0.4 and 0.8, respectively. The adjustment of the interaction of a CO_2 molecule with the SiO_2 surface by assigning the change to the electrostatic part of the interaction is to some extent arbitrary. The simulations show that the averaged total gas–solid interaction energy obtained from the TTAM potential at a relative pressure of 0.3 is -25.2 kJ/mole whereas the error bar point at the same surface coverage given by the reduced charge version of the potential gives a total average energy of -19.9 kJ/mole. At this coverage, the total simulated gas–solid energy for the TTAM potential is comprised of an electrostatic term amounting to -12.4 kJ/mole and a dispersion/repulsion part amounting to -12.8. Note that the average electrostatic energy is not strictly proportional to the charges because the averaging process gives somewhat different positions and orientations for different potentials. Thus, a change in the average total energy amounting to roughly 20% is produced by a change in the SiO_2 charges amounting to 30%. Several possible reasons for the need for this adjustment of the CO_2–SiO_2 potential to give agreement with experiment can be suggested. For instance, the van der Waals part could be given somewhat incorrectly by our estimates. Furthermore, the use of discrete charge models for the continuous charge distributions in CO_2 and in SiO_2 is an oversimplification[24] that could give incorrect electrostatic energies. Also, if the electrostatic field at the surface is sufficiently strong, the adsorbed CO_2 molecules will be polarized; any effects of this polarization upon the CO_2–CO_2 energies has been omitted here. Adsorption studies of other gases on these surfaces should help clarify the question of the proper gas–solid and gas–gas potentials for these systems.

The simulated isotherms on the surfaces *C* and *D* coincide at small values of relative pressures but diverge at coverages greater than roughly 0.3 monolayer. The divergence is much larger than standard deviations of the data for the isotherm on surface *D* given in Fig. 4 (for other isotherms the standard deviations are not shown but they are of the same magnitude). At this stage, we can not speculate on how this divergence is connected to the difference in the atomic structures of the respective surfaces.

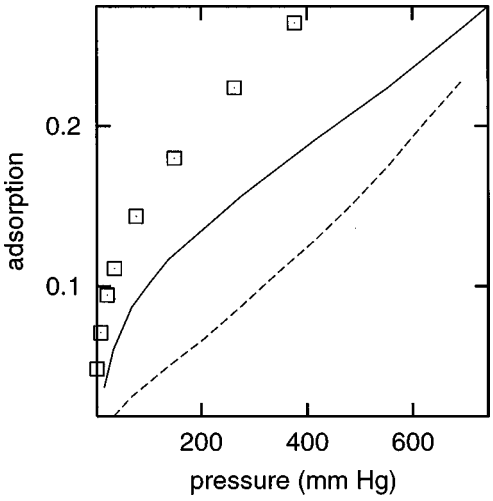

FIG. 6. Experimental isotherms of adsorption of CO_2 at 194.5 K. Solid line: hydroxylated nonporous silica; dashed line: dehydroxylated nonporous silica; symbols: glass fiber. Adsorption is in cc S.T.P./m^2.

The experimental isotherms of CO_2 on silica presented in Fig. 6 are the same as those in Fig. 4 but are compared with isotherms measured on glass fibers. The glass fiber isotherm lies higher than the isotherms on the silica surfaces. In line with our previous arguments, this difference should be ascribed to the difference between the surface atomic structures but the situation is more complicated now because we have to compare the surface structures for the different chemical compositions of silica and *E*-glass. Besides, the surface of the glass fiber is hydroxylated to some unknown degree. Still, the experimental CO_2 adsorption is greater even than that on a hydroxylated silica surface. The difference is nearly as large as that between isotherms on the *B* and *C* or *D* surfaces in Fig. 4, which suggests that the surface of the glass fiber differs considerably from that of pure hydroxylated silica.

IV. CONCLUSION

We have shown that the isotherm of CO_2 is a sensitive probe of the atomic structure of amorphous silica surface while the isotherm of Ar is relatively insensitive to that structure. In our previous paper we showed that the distribution of the charged atomic species on a weakly annealed model silica surface can give considerable concentrations of singly and triply coordinated oxygen atoms that correspond to strong hydrophilic adsorption sites while an extensively annealed surface (*C*) is characterized by different arrangements of these species which give rise to a surface that is hydrophobic, in agreement with experiment.[5] In this paper, a quantitative comparison of simulated and experimental adsorption characteristics of carbon dioxide on those surfaces has been made that confirms our previous suggestion concerning the atomic structures of vitreous silica surfaces: The weakly annealed model surfaces (*A* and *B*) that have considerable concentrations of singly and triply coordinated oxygen atoms generate isotherms and heats of adsorption which differ considerably from the experimental systems considered here but the extensively annealed model silica surfaces (*C*

and *D*) composed only of bridging oxygen atoms generate adsorption characteristics close to experiment. This validates the simulated atomic structure of surfaces *C* and *D* and emphasizes the importance of thorough annealing[6] in computer simulation of amorphous silica and silicate glass surfaces.

In future work, simulations of other molecules with varying polarities adsorbed on these simulated silica surface with be carried out in an effort to better characterize the effects of surface structure upon adsorption. Other simulated surfaces will also be considered including those of hydroxylated silicas and silicate glasses.

ACKNOWLEDGMENT

Support for this research was provided by Grant No. DMR 9803884 of the Division of Material Research of the NSF.

[1] A. C. Wright, J. Non-Cryst. Solids **179**, 84 (1994).
[2] P. H. Poole, P. F. McMillan, and G. H. Wolf, in *Structure, Dynamics and Properties of Silicate Melts*, edited by J. F. Stebbins, P. F. McMillan, and D. B. Dingwell [Rev. Mineral. **32**, 563–616 (1995)].
[3] B. P. Feuston and S. H. Garofalini, J. Chem. Phys. **91**, 564 (1989).
[4] *The Surface Properties of Silicas*, edited by A. P. Legrand (Wiley, New York, 1998).
[5] V. A. Bakaev and W. A. Steele, J. Chem. Phys. **111**, 9803 (1999), preceding paper.
[6] V. A. Bakaev, Phys. Rev. B (to be published).
[7] S. Tsuneyuki, M. Tsukada, H. Aoki, and Y. Matsui, Phys. Rev. Lett. **61**, 869 (1988).
[8] D. A. Payne, K. S. W. Sing, and D. H. Turk, J. Colloid Interface Sci. **43**, 287 (1973).
[9] N. O. Lemcoff and K. S. W. Sing, J. Colloid Interface Sci. **61**, 227 (1977).
[10] M. P. Allen and D. J. Tildesley, *Computer Simulation of Liquids* (Clarendon, Oxford, 1987).
[11] D. Frenkel and B. Smit, *Understanding Molecular Simulation* (Academic, San Diego, 1996).
[12] E. J. Bottani and V. A. Bakaev, Langmuir **10**, 1550 (1994).
[13] K. Watanabe, N. Austin, and M. R. Stapleton, Mol. Simul. **15**, 197 (1995).
[14] S. J. Gregg and K. S. W. Sing, *Adsorption, Surface Area and Porosity*, 2nd ed. (Academic, London, New York, 1982).
[15] W. H. Press, S. A. Teukolsky, W. T. Vetterling, and B. P. Flannery, *Numerical Recipes in FORTRAN* (Cambridge University Press, Cambridge, UK, 1992).
[16] R. G. Della Valle and H. C. Andersen, J. Chem. Phys. **97**, 2682 (1992).
[17] J. O. Hirschfelder, C. F. Curtiss, and R. B. Bird, *Molecular Theory of Gases and Liquids* (Wiley, New York, 1954), p. 1110.
[18] A. Lotfi, J. Vrabec, and J. Fischer, Mol. Phys. **76**, 1319 (1992).
[19] J. G. Harris and K. H. Yung, J. Phys. Chem. **99**, 12021 (1995).
[20] *International Thermodynamic Tables of the Fluid State: Carbon Dioxide*, edited by S. Angus *et al.* (Pergamon, Oxford, 1976), Vol. 3.
[21] A. Magnus and W. Kälberer, Z. Anorg. Allg. Chem. **164**, 357 (1927).
[22] N. N. Avgul' *et al.*, Kolloidn. Zh. **36**, 928 (1974) [English translation Colloid. J. of the USSR **36**, 841 (1974)].
[23] A. Hirotani *et al.*, Appl. Surf. Sci. **120**, 81 (1997).
[24] A. J. Stone, *The Theory of Intermolecular Forces* (Clarendon, Oxford, 1996).